The American Journal of Pathology, Vol. ■, No. ■, ■ 2022

ELSEVIER

The American Journal of PATHOLOGY

ajp.amjpathol.org

Platelet Endothelial Cell Adhesion Molecule (PECAM/CD31) Blockade Modulates Neutrophil Recruitment Patterns and Reduces Infarct Size in Experimental Ischemic Stroke

Neil A. Nadkarni,* Erika Arias,† Raymond Fang,‡ Maureen E. Haynes,† Hao F. Zhang,‡ William A. Muller,† Ayush Batra,*† and David P. Sullivan†

From the Departments of Neurology, Pathology,† and Biomedical Engineering,‡ Northwestern University, Chicago, Illinois*

Accepted for publication July 14, 2022.

Address correspondence to David P. Sullivan, Department of Pathology, Northwestern University, Ward Bldg. 3-070, 303 E. Chicago Ave., Chicago, IL 60611.
E-mail: d-sullivan@northwestern.edu.

The infiltration of polymorphonuclear leukocytes (PMNs) in ischemia-reperfusion injury (I/RI) has been implicated as a critical component of inflammatory damage following ischemic stroke. However, successful blockade of PMN transendothelial migration (TEM) in preclinical studies has not translated to meaningful clinical outcomes. To investigate this further, leukocyte infiltration patterns were quantified, and these patterns were modulated by blocking platelet endothelial cell adhesion molecule-1 (PECAM), a key regulator of TEM. *LysM-eGFP* mice and microscopy were used to visualize all myeloid leukocyte recruitment following ischemia/reperfusion. Visual examination showed heterogeneous leukocyte distribution across the infarct at both 24 and 72 hours after I/RI. A semiautomated process was designed to precisely map PMN position across brain sections. Treatment with PECAM function-blocking antibodies did not significantly affect total leukocyte recruitment but did alter their distribution, with more observed at the cortex at both early and later time points (24 hours: 89% PECAM blocked vs. 72% control; 72 hours: 69% PECAM blocked vs. 51% control). This correlated with a decrease in infarct volume. These findings suggest that TEM, in the setting of I/RI in the cerebrovascular, occurs primarily at the cortical surface. The reduction of stroke size with PECAM blockade suggests that infiltrating PMNs may exacerbate I/RI and indicate the potential therapeutic benefit of regulating the timing and pattern of leukocyte infiltration after stroke. *(Am J Pathol 2022, ■: 1–14; https://doi.org/10.1016/j.ajpath.2022.07.008)*

Ischemic stroke is a leading cause of morbidity and mortality in the world.[1] Current stroke reperfusion therapies are restricted to tissue plasminogen activator and/or mechanical thrombectomy based on select criteria and time constraints.[2,3] However, some patients do poorly despite treatment with thrombectomy.[4,5] These poor outcomes are thought to be a result of ischemia/reperfusion injury (I/RI), a consequence of restoring blood flow to ischemic tissue that places potentially salvageable penumbra (the area of moderately reduced blood flow) at risk for irrevocable damage.[6,7] I/RI thus increases the amount of tissue damage from the initial insult. I/RI increases local inflammatory cytokine release, up-regulates endothelial cell adhesion molecules, and ultimately facilitates infiltration of leukocytes into brain parenchyma.[8–11] This infiltration of leukocytes is known as transendothelial migration (TEM), the step in leukocyte emigration in which the leukocyte leaves the blood vessel to carry out its role in the inflammatory response.[12–16] Defining the patterns and implications of leukocyte recruitment in stroke-related I/RI and TEM may ultimately translate to improved outcomes.

Imaging performed at the Northwestern University Center for Advanced Microscopy, supported by CCSG P30 CA060553 awarded to the Robert H. Lurie Comprehensive Cancer Center. Supported by NIH grants R25 NS070695 (N.A.N.), T32 GM142604 (R.F.), and R35 HL155652 (W.A.M.).

N.A.N. and E.A. contributed equally to this work.

Disclosures: None declared.

https://doi.org/10.1016/j.ajpath.2022.07.008

In the stereotyped leukocyte recruitment cascade, polymorphonuclear leukocytes (PMNs) are the first leukocyte subtype to be recruited to a site of inflammation.[17,18] However, the location and timing of their recruitment in response to ischemic stroke are not settled.[19,20] The molecular components that mediate trafficking during cerebral I/RI are largely unknown.[21] Several preclinical studies affirm that PMNs do enter the brain parenchyma, whereas other studies report they never leave the perivascular space.[19,22,23] One major study states PMNs do enter some severely ischemic brains from the meningocortical surface but only after 12 to 24 hours.[20] It is even unclear whether the recruitment of PMNs is detrimental to I/RI after stroke because PMNs can also have beneficial roles in the inflammatory response.[24–27] Some preclinical studies have shown that PMN depletion reduces infarct size and ameliorates functional outcomes, whereas other studies show no effect on stroke volume.[28–32] A reappraisal of the current knowledge with attention to both spatial and temporal attributes of leukocyte recruitment in I/RI will help clarify these conflicting results.

Most of the published studies use representative high magnification confocal imaging to study PMN infiltration. Although this technique provides high resolution in a particular region, it does not provide a cohesive spatiotemporal image of leukocyte recruitment across the whole brain. As a result, the big picture of how and when leukocytes are recruited in the post-stroke brain is incomplete. Second, many preclinical stroke studies do not target the PMN response during the dynamic time course of their response following I/R and use one time point after I/RI to look at their outcome of interest.[30–32] These disconnects may explain why PMN blockade strategies—often successful in preclinical models—have not translated to success in clinical trials. These translational roadblocks are likely due to an incomplete understanding of how dynamically leukocyte recruitment patterns change throughout I/RI both spatially and temporally.

Homophilic engagement of platelet endothelial cell adhesion molecule-1 (PECAM-1) on PMNs with PECAM at endothelial cell borders is required for TEM in systemic inflammation models.[33–36] This study sought to identify how blocking PECAM function would modulate leukocyte recruitment resulting from I/RI across the entire infarct both spatially and temporally. Previous work in other models of inflammation and neuroinflammation revealed that blocking TEM with function-blocking antibodies modulates leukocyte recruitment and improves outcomes.[37,38] Described here is a method to precisely define and quantify leukocyte spatial location. I/RI was examined at both 24 hours and 72 hours after stroke to understand how disrupting TEM would change leukocyte infiltration patterns across time points. The application of this methodology allows for precise delineation of leukocyte infiltration patterns and how they change dramatically over time throughout I/RI. Furthermore, this study confirms that disrupting PECAM function modulates these patterns and reduces stroke infarct size.

Materials and Methods

Mice

All procedures were carried out with the approval of the Institutional Animal Use and Care Committee of Northwestern University (Public Health Service assurance number A328301). Mice were housed in the institutional animal facility operated by the Northwestern University Center for Comparative Medicine in Chicago, IL, and were maintained according to standard Association for Assessment and Accreditation of Laboratory Animal Care protocols. The FVB/n *LysM-eGFP* strain was derived by backcrossing C57BL/6 *LysM-eGFP* mice into wild-type FVB/n mice (Jackson Laboratory, Bar Harbor, ME) for nine generations as described previously.[39] The myelomonocytic cells of these mice were rendered fluorescent due to the expression of enhanced green fluorescent protein (GFP) under the *lysozyme M* (*LysM*) locus. Heterozygous *LysM-GFP* mice of both sexes weighing 25 to 35 g and aged 3 to 4 months were used for all experiments. *Catchup*^{IVM} mice have been previously described and were used to generate bone-marrow chimeras by transferring the heterozygotes (for both alleles) into wild-type C57BL/6 recipients as previously described.[40,41] To minimize the disruption to the brain, these mice were head shielded during the irradiation.

tMCAO Model

All procedures followed the ARRIVE guidelines with aseptic surgical technique and continuous monitoring to ensure body temperature of 37°C ± 0.5°C. Mice were subjected to transient middle cerebral artery occlusion (tMCAO) according to the Koizumi method.[42–44] Briefly, mice were anesthetized (isoflurane 3% v/v) and pretreated with 0.05 mg/kg s.c. buprenorphine to minimize pain. Lubricant was placed on both eyes, and 0.5 mL of saline was injected for hydration. A midline ventral neck incision Q9 (approximately 1.5 cm) was made to expose the common carotid, which was ligated. A weight-matched silicon coated monofilament (Doccol 602245 if <30 g, 602345 if >30 g; Doccol, Sharon, MA) was inserted through an aperture Q10 made approximately 2 mm caudal to the carotid bifurcation. The monofilament was advanced approximately 9 mm past the bifurcation of the internal and external carotid arteries to occlude the middle cerebral artery for 90 minutes. A security knot was placed at the bifurcation to prevent premature retraction. With the middle cerebral artery still occluded, the incision was closed, and the mouse was allowed to recover from anesthesia in a heated cage. Sham surgeries were conducted with the same surgical procedure, however without the advancement of the monofilament. For clinical translatability, mice were assessed for behavior during the intraischemic period. Mice were included for further studies if evidenced to have decreased contralateral whisker response, contralateral curling when lifted by the tail, and

FLA 5.6.0 DTD ■ AJPA3771_proof ■ 19 August 2022 ■ 6:39 pm ■ EO: AJPA-D-22-00074

contralateral circling. Just prior to reperfusion at 90 minutes, the mouse was reanesthetized and injected intravenously with 100 μg of either blocking PECAM antibody (Armenian hamster anti-mouse, clone 2H8 described in Bogen et al[45]) or isotype control (Jackson ImmunoResearch Laboratories, West Grove, PA). The incision was then opened again, and the filament was removed to ensure reperfusion with subsequent resuture of the ventral incision. Mice that did not meet the intraischemic inclusion criteria or that did not follow the usual recovery time course after surgery were excluded. Mice were monitored daily; those displaying signs of excessive pain, or poor grooming or health, were excluded because these behaviors correlate with subarachnoid hemorrhage, incomplete reperfusion, or inadequate occlusion (approximately 30% of mice were excluded). Behavior exclusion criteria were preceded by laser speckle contrast imaging, which was initially utilized to confirm sufficient occlusion and reperfusion. Mice that were subjected to the 72-hour time point were given booster doses of either isotype control or blocking PECAM antibody every 24 hours via i.v. injection.

Brain Tissue Prep

Experimental endpoints for this study were 24 hours and 72 hours after occlusion. Immediately prior to sacrifice, mice were injected intravenously (r.o.) with nonblocking PECAM antibody to label vasculature (clone 390, purchased from EMD Millipore, Billerica, MA), fluorescently conjugated with DyLight 650 (Thermo Fisher Scientific, Waltham, MA) according to the manufacturer's instructions. This antibody binds PECAM at a different epitope (domain 5) than the blocking PECAM antibody and does not interfere with its function or susceptibility to blocking antibody.[39,46] Mice with vessels that were unable to be visualized with nonblocking PECAM antibody indicated lack of reperfusion and were subsequently excluded. Mice were subjected to deep anesthesia via isoflurane inhalation and subsequently subject to thoracotomy and transcardial perfusion with 30 mL of phosphate-buffered saline until blood cleared. Mice were then decapitated, and the brain was removed from the skull. Mice with a subarachnoid hemorrhage were excluded from studies. Brains were placed in a murine brain matrix (RWD, San Diego, CA), cut in 2-mm intervals, and placed in 1% triphenyltetrazolium chloride (TTC) for 20 minutes at room temperature. At this point, brain slices were placed in 4% paraformaldehyde overnight and subsequently sucrose dehydrated over the following 48 hours. Slices were imaged within 72 hours of animal sacrifice.

Microscopy

For confocal microscopy, high-resolution images of brain tissue were collected using an UltraVIEW VoX imaging system (PerkinElmer, Naperville, IL) equipped with a Yokogawa CSU-1 spinning disk (Yokogawa, Sugar Land, TX) and a 40× oil-immersion objective (1.00 numerical aperture). Images were collected using Volocity software version 6.5.1 (PerkinElmer) and analyzed using Fiji software version 1.53F51.[47]

For wide-field microscopy, brain slices were placed on coverslip dishes and imaged on a Nikon Eclipse Ti2 wide-field microscope (Nikon, Tokyo, Japan) with a Nikon 4× Q14 objective (0.20 numerical aperture) equipped with a Nikon DS-Qi2 camera. Images were collected over the entire slice with a 15% overlap and stitched together using the embedded stitching algorithm of NIS-Elements software version 5.11.01 (Nikon) with the Optimal Path option. For general display and heatmap generation, individual channels were separated in Fiji and subjected to rolling ball background (radius of 10 μm for the GFP leukocyte channel and 5 μm for the vessel channel). Channels were then recombined and contrast adjusted for better display. To render the images for heatmaps, the leukocyte GFP image was subjected to a Gaussian blur of 50 μm in Fiji and then rendered with the generic Fiji heatmap lookup table. To preserve intensity differences for the heatmap rendition and facilitate direct comparison between images, the maximum value in the brightest region of all the images was set to the hottest color (white). These min/max values were propagated to the other images.

Processing and Segmentation Algorithm for Leukocyte Position

The raw wide-field images were separately processed to identify and segment all fluorescent cells and determine their position relative to the brain surface boundary. The segmentation of cells and the delineation of their boundaries were performed using the PyImageJ and scikit-image libraries of Python software version 3.7.[48]

For cell segmentation, the cell channel was loaded into ImageJ software version v1.53q (NIH, Bethesda, MD; Q15 *https://imagej.nih.gov*)[47] via PyImageJ v1.0.2 wraparound (*https://zenodo.org/record/5537065#.YvS5tRzMKUk*). Max Q16 intensity projection in the depth dimension, Gaussian blur with a sigma of 0.826 μm, and rolling ball background subtraction with a radius of 16.52 μm was done as preprocessing steps to generate better contrast between cells and the nonuniform background. Stable count thresholding was applied to compute a threshold differentiating cells from background,[49] with manual corrections to the threshold performed as needed. To separate overlapping clusters of cells, marker-based watershed transform was utilized.[50] The diffraction of light leads to the blurring of cell boundaries, with the space between cells having a signal greater than the threshold used to segment the cells. However, thresholding alone is not sufficient to separate cells that are too closely clustered, even though local maxima can be used to identify the location of different cells within each cluster. Based on these observations, a Laplacian of Gaussian filter, commonly used in blob

FLA 5.6.0 DTD ■ AJPA3771_proof ■ 19 August 2022 ■ 6:39 pm ■ EO: AJPA-D-22-00074

detection, was applied with a sigma of 4.67 μm to amplify the signal of local maxima.[51] For each cell cluster, the negative of the Laplacian of Gaussian signal was quantized to have values 0 and 20 with the minimum Laplacian of Gaussian signal of each cluster being assigned a value of 0 and the maximum signal being assigned a value of 20 to smooth the image as reported elsewhere in the literature.[52] Nonmaximal suppression[53] with a radius of 4.67 μm was applied to the quantized Laplacian of Gaussian image, and the subsequent local maxima were set as markers for the marker-based watershed transform. The different basins of the marker-based watershed transform were used to separate each cell cluster, with pixels of each cell in a cluster belonging to different basins. Connected regions with an area less than an area of 5.45 μm^2, corresponding to a quarter of the area of a circle with a radius of 4.67 μm, were excluded and considered as noise. Additionally, particles erroneously identified as cells (such as lint and large debris) were manually removed from the segmented cells.

The brain boundary was determined by thresholding the vessel channel. A manual threshold differentiating the brain from background was applied, and the largest connected component was used to segment brain tissue. Rarely, regions of interest were drawn in Fiji as necessary to correct for any errors in the segmented brain tissue, with the option of including or excluding any region of interest from the segmented brain tissue. Boundaries of the segmented brain tissue were taken to be the brain boundary.

Following cell and boundary segmentation, the distance transform was applied to the brain boundary to determine the distance of each of the pixels in the image from the boundary.[54] A region of interest was drawn to denote the infarcted hemisphere and only cells within this region were included in the subsequent analysis. Additionally, cells outside of the brain boundary were excluded from the analysis. The centroid of every segmented cell was computed and the spatial position of each of the centroids was linearly interpolated to the distance transform grid to determine the distance of each of the cells from the boundary of the brain. The distances of every cell from the brain boundary were saved and used for further analysis. Calculation of the cell centroids and distance transform was done using the image processing toolbox of MATLAB software version R2020a (MathWorks, Natick, MA).

Flow Cytometry and Quantitation

Cells for flow cytometry were obtained from separated hemispheres of phosphate-buffered saline–perfused, TTC-stained brains. Individual hemispheres were digested for 30 minutes at 37°C in Accutase (00 to 4555-56; Thermo Fisher Scientific), filtered through a 100-μm strainer, and then centrifuged in a Percoll (P1644; Sigma-Aldrich, St. Louis, MO) gradient as previously described.[55] Central nervous system cells were stained with: CD45, CD11b, TMEM119, Ly6C, Ly6G, and a LIVE/DEAD cell stain (Thermo Fisher Scientific) (Table 1 lists the flow cytometry reagents). [T1] CountBright absolute counting beads (cat. C36950; Thermo Fisher Scientific) were used according to the manufacturer's instructions to obtain the absolute number of cells. Flow cytometry was performed on a LSRFortessa X-20 cytometer (BD Biosciences, Franklin Lakes, NJ). Data were analyzed by FlowJo software version 10.8.1 (FlowJo, Ashland, OR). Q18

Statistical Analysis

Where indicated, averaged data (ie, infarct volume, cell counts, and mean position from the surface) were analyzed using an unpaired single factor analysis of variance to identify statistically significant differences. For comparison Q19 of the cell position data between different time points and treatment groups, data were analyzed using the rank-sum test due to non-normality of data as determined by the Shapiro-Wilk normality test. Statistical analysis was performed in R Studio software version 4.1.1 (R Foundation for Statistical Computing, Vienna, Austria). Q20

Results

Leukocytes Are Distributed Heterogeneously across the Infarct Post-Stroke

In a typical/generic inflammatory response, PMNs are initially recruited to the site of inflammation during the first 24 hours. By 72 hours, they would be replaced largely by monocytes. To easily examine recruitment and distribution of both groups that resulted from an ischemic insult, *LysM-GFP* reporter mice, which express GFP in all myelomonocytic leukocytes (PMNs and monocytes) were used. All

Table 1 Reagents Used for Flow Cytometry

Catalog number	Target	Fluorophore	Company
562127	CD11b	V500	BD Bioscience
127608	Ly6G	PE	BioLegend (San Diego, CA)
103132	CD45	PerCP/Cyanine5.5	BioLegend
25611982	TMEM119	PE-Cyanine7	Thermo Fisher Scientific
128049	Ly6C	BV650	BioLegend
C36950	CountBright Absolute Counting Beads		Thermo Fisher Scientific
553142	Purified Rat Anti-Mouse CD16/CD32 (Mouse BD Fc Block)		BD Pharmingen (San Diego, CA)
L 34964	LIVE/DEAD Fixable Violet Dead Cell Stain	BV420	Thermo Fisher Scientific

FLA 5.6.0 DTD ■ AJPA3771_proof ■ 19 August 2022 ■ 6:39 pm ■ EO: AJPA-D-22-00074

mice used were heterozygous for the *LysM* locus so that their leukocytes would retain a functional copy of *LysM*. Furthermore, to better examine the function of PECAM, the FVB/n strain, which has been shown to more closely mimic human physiology with regard to PECAM function,[39,56,57] was used.

Mice were subjected to tMCAO and reperfused after 90 minutes; 72 hours after reperfusion, animals were injected with fluorescent non−function-blocking anti-PECAM antibodies to label the vasculature. Animals were then sacrificed and perfused with phosphate-buffered saline, and brains were harvested, sliced, and then stained with TTC to identify infarcted regions (Figure 1A). Using wide-field microscopy, images of entire slices that contained the core of the infarct were collected, compiled, and then stitched together (a representative nonprocessed image is shown in Figure 1B).

Examining different regions across the section showed a striking amount of heterogeneity, even within seemingly similar regions of infarct, such as along the cortical surface, for example. It was expected that some general regions would be more populated than others (ie, cortical versus subcortical) (Figure 1, C and D) and that this could vary as a function of time. Indeed, qualitatively the density of GFP-positive cells in the cortex was different from the subcortex, particularly at 24 hours (described quantitatively below). However, even within the infarct (as defined by absent TTC staining), leukocyte numbers varied markedly and in a seemingly random way. As expected though, GFP-positive myelomonocytic cells were rarely found in the peri-infarct region (<100 μm from the red-white TTC border) (Figure 1E) or the contralateral side of the brain (Figure 1F), suggesting that their recruitment to the infarct is at least a result of local signals specific to the insult.

Number of PMNs Increases over Time in Acute I/RI

PMNs are typically the first responders to tissue damage in most models of inflammation, with monocytes replacing them by later time points, at 48 to 72 hours. The precise recruitment and timing of these leukocyte subtypes in response to stroke is not settled. To help bring some clarity to this and to better understand the subtypes recruited in this model, flow cytometry was used to define neutrophil and monocyte populations in the *LysM-GFP* mice at 24 hours and 72 hours after reperfusion. Single-cell suspensions of the ipsilateral and contralateral hemispheres were prepared and labeled for analysis. PMNs were defined as TMEM119^{-}, CD11b^{+}, Ly6G^{+}, and GFP^{+}, whereas monocytes were defined as TMEM119^{-}, CD11b^{+}, Ly6G^{-}, Ly6C^{high}, and GFP^{+} (gating strategy in Supplemental Figure S1). The inclusion of GFP^{+} was largely redundant because virtually all PMNs and monocytes were GFP-positive and all the GFP-positive cells were either PMNs or monocytes. Also, relatively few resident macrophages were GFP-positive because almost no GFP-positive cells were detected on the nonischemic side (Figure 1B) or in control brains (*LysM-GFP*−positive mouse, no surgery, data not shown).

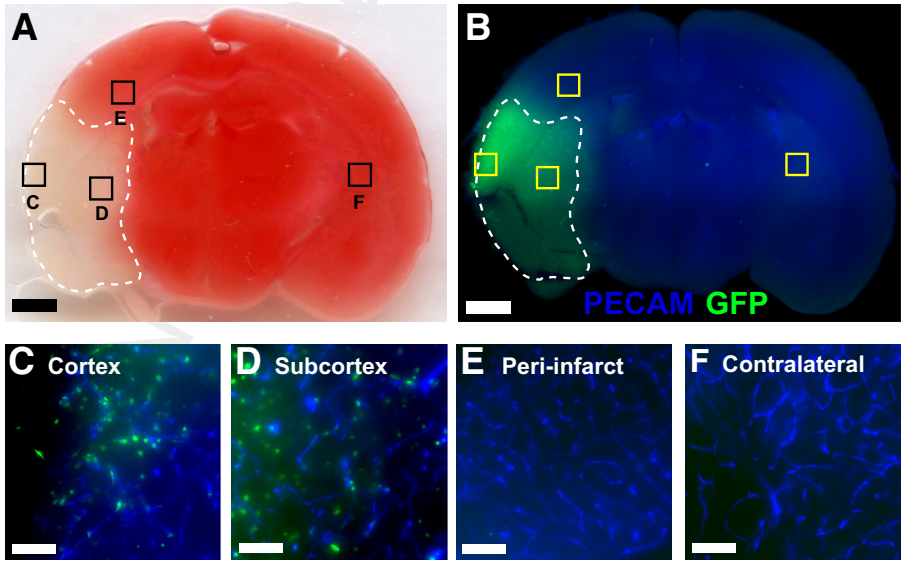

Figure 1 Leukocyte infiltration in various regions of the brain after stroke. **A:** *LysM-GFP* mice were subjected to an ischemic stroke according to *Materials and Methods*, and reperfused after 90 minutes; 24 hours after reperfusion, the mouse was injected with a fluorescent-vessel labeling antibody and sacrificed. The brain was harvested, sliced, stained with triphenyltetrazolium chloride (TTC), and then imaged. The **dashed line** denotes infarct boundary as determined by TTC. **B:** The same brain slice was imaged using fluorescence microscopy. **Yellow boxes** are the same region as those denoted in **black boxes** in **A**. PECAM (blue) denotes vessels, and green fluorescent protein (GFP) (green) denotes *LysM-GFP*−positive leukocytes (**B-F**). The composite image of the entire slice was assembled according to *Materials and Methods*. **C-F:** Various regions (marked in **A**) across the slice are shown at higher resolution. Representative images of a typical brain are shown. Scale bars: 1 mm (**A** and **B**); 100 μm (**C-F**). Original magnification: 4× (**A** and **B**).

FLA 5.6.0 DTD ■ AJPA3771_proof ■ 19 August 2022 ■ 6:39 pm ■ EO: AJPA-D-22-00074

It was expected that the majority of cells recruited at 24 hours would be PMNs and that these would largely be replaced by monocytes by 72 hours. Indeed at 24 hours, more than 75% of the recruited cells to the ipsilateral hemisphere were PMNs (Figure 2). However, the number of PMNs recruited more than doubled by the 72-hour time point, indicating that PMNs are recruited well past 24 hours. Furthermore, an increase in the number of monocytes recruited was observed from 24 to 72 hours, but even at 72 hours, they numbered roughly equal to PMNs. Treatment with PECAM function-blocking antibodies did not significantly affect the recruitment of either PMNs or monocytes at either time point (data not shown). This was expected because PECAM is known to function at the TEM step and not the initial adhesion steps, which results in an accumulation of leukocytes arrested inside the vessel.[39]

Recruitment of leukocytes to the contralateral hemisphere was more than an order of magnitude less than the ipsilateral hemisphere and on par with the numbers of myeloid cells observed in the sham controls, with the notable exception of the 24-hour time point, which showed a slight increase in both PMN and monocyte recruitment compared with sham (data not shown).

PECAM Blockade during Stroke I/RI Arrests Leukocytes inside Vessels

Many reports describe the disruption of TEM on a granular and local scale but neglect to examine effect across the insult on a global scale. To block TEM as early as possible in the I/RI time course and in a clinically relevant manner, blocking PECAM antibody was administered immediately prior to reperfusion. To maintain the block for 72 hours, blocking PECAM antibody was readministered daily via i.v. injections. Both 24-hour and 72-hour time points were studied to define how PECAM blockade altered the natural history of leukocyte migration and whether this had an effect on stroke volume. Toward this end, upon sacrifice at 24 hours or 72 hours, the entire surface of a slice through the core of the infarct at the level of the bregma was imaged using both confocal microscopy and wide-field microscopy to understand the granular and global effects of anti-PECAM on leukocyte distribution in the stroked brain.

In most vascular beds, leukocyte TEM is restricted to post-capillary venules. PECAM is a key signaling molecule in this process and functions via homophilic interactions between the endothelial cell and the migrating leukocyte. Except for some inflammatory models particularly in C57Bl/6 mice, PECAM is required for the TEM, regardless of the leukocyte subtype or vascular bed.[56] The authors hypothesized that disrupting PECAM function would block the TEM of leukocytes recruited as a result of I/RI. When leukocyte position was examined using lower-power wide-field microscopy, leukocytes were found mostly outside vessels, whereas in PECAM-blocked vessels, many more were found overlapping vessels (Figure 3A). Because

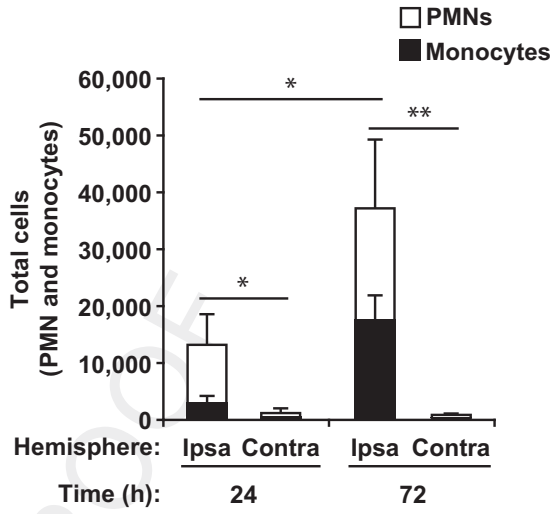

Figure 2 Polymorphonuclear leukocytes (PMNs) infiltrate the infarcted hemisphere at 24 hours, whereas monocytes arrive later. *LysM-GFP* mice were subjected to transient middle cerebral artery occlusion and reperfused after 90 minutes. Ipsilateral (Ipsa) and contralateral (Contra) hemispheres were harvested at either 24 or 72 hours after reperfusion. Single-cell suspensions were prepared and labeled for flow cytometry according to *Materials and Methods*. Total cell counts were calculated using counting beads. PMNs and monocytes were gated according to a standard strategy (detailed in Supplemental Figure S1). The total GFP-positive leukocytes (PMNs and monocytes) are shown along with the number of each cell type. *P* values indicate significance within each leukocyte subtype (ie, both PMN and monocytes numbers were separately statistically significant for 24 hours compared with 72 hours). Data are expressed as means ± SD. $n = 3$ mice for each time point. $^{*}P < 0.05$, $^{**}P < 0.01$.

wide-field imaging has limited resolution in the *z* axis, high-power confocal microscopy was used for improved resolution. Indeed, in control samples, GFP-positive cells were mostly observed outside of vessels at both 24 and 72 hours (Figure 3B). Often times, they were more than 20 μm away from the vessel and therefore likely outside of the perivascular space. Interestingly, after injection of PECAM function-blocking antibodies, substantially more GFP-positive cells were found inside vessels at 24 hours (79% outside in control versus 45% in PECAM blocked; Figure 3B shows a representative leukocyte inside the vessel). However, this did not persist at the 72-hour time point, because most were found outside vessels similar to the control, even though the mice were boosted daily with additional PECAM blocking antibodies (data not shown). This suggests that although PMN TEM can be blocked early in stroke (24 hours), there may be mechanisms of evasion for PECAM blockade as time progresses (72 hours).

PECAM Blockade in Stroke Modulates Leukocyte Recruitment Patterns and Reduces Lesion Size throughout I/RI

To precisely define the effect of PECAM blockade on PMN position in the infarcted brain on a more global scale, the brain slices were first stained with TTC to delineate and

FLA 5.6.0 DTD ■ AJPA3771_proof ■ 19 August 2022 ■ 6:39 pm ■ EO: AJPA-D-22-00074

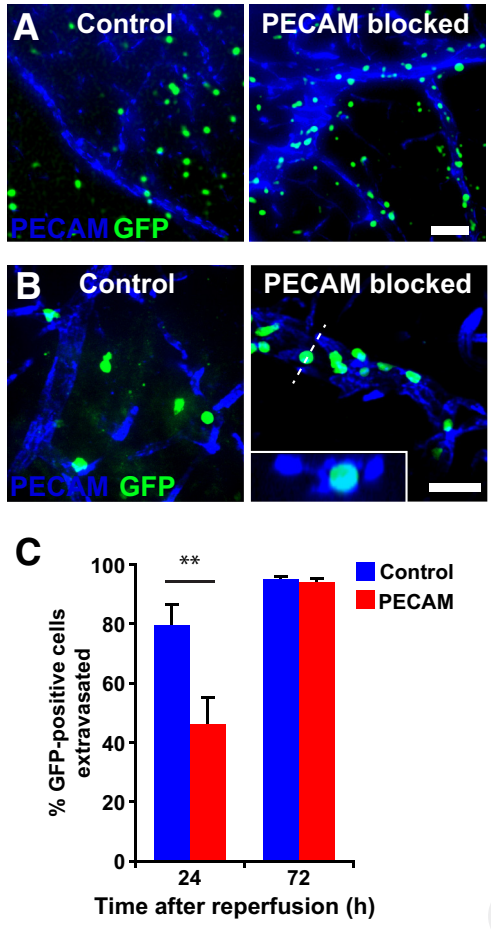

Figure 3 Blocking PECAM function retains leukocytes inside blood vessels. **A:** *LysM-GFP* mice were subjected to transient middle cerebral artery occlusion and reperfused after 90 minutes. Immediately after reperfusion, mice were injected with either control or PECAM function-blocking antibodies via i.v. injection. Twenty-four hours after reperfusion, the mice were injected with a fluorescent-vessel labeling antibody and sacrificed after 30 minutes. The brains were harvested, sliced, and then imaged with wide-field imaging. Images were collected across the entire brain, but regions at the cortical surface are shown. Note that many green fluorescent protein (GFP)-positive cells are observed near or inside the vessels when PECAM is blocked. **B:** These brains were also imaged using confocal fluorescence microscopy at a magnification that allows for the precise determination of the leukocyte's position relative to the vessel. **Inset** shows an orthogonal view through the vessel at a position indicated by the **dashed line** and displays a typical leukocyte inside a vessel. Representative images are shown. **C:** The exact position of GFP-positive leukocytes relative to the vessel was quantified from orthogonal views. Leukocytes were scored inside the vessel if the majority of the cell body was inside the vessel. Data are expressed as means ± SD. $n = 4$ fields; $n = 4$ mice per field; $n > 40$ cells per mouse. $^{**}P < 0.01$. Scale bars: 100 μm (**A**); 50 μm (**B**). Original magnification: 4× (**A**); 40× (**B**).

quantify the infarct (Figure 4, A and B). A series of fluorescence images were then acquired across the entire brain slice and stitched together to create one large high-resolution image of the entire sample (Figure 4, C and D). Even though there was increased background signal in the infarct (largely due to changes in tissue autofluorescence), GFP-positive cells were easily distinguished from the noise (Figure 1A). Because individual GFP-positive leukocytes are difficult to distinguish in a zoomed-out view, the image was rendered as a heatmap so that the density and location of the infiltrating GFP-positive leukocytes could be more fully appreciated (Figure 4, E and F). Leukocyte hot spots were more easily seen in this rendition, although there was no consistent pattern observed between animals. At 72 hours, there were still many GFP-positive cells near the cortical surface, but a significant fraction was observed deeper and spread throughout the cortex and subcortex (Figure 4E). By contrast, blocking PECAM function with antibodies appeared to shift the GFP-positive population to a more superficial distribution (Figure 4F) [a more dispersed and deeper distribution is observed in the control (Figure 4E) compared with the PECAM-blocked sample (Figure 4F)]. Interestingly, this also correlated with a statistically significant, albeit modest, decrease in the infarct volume at both 24 and 72 hours (24 hours: 26% of cerebral volume compared with 17%, $n = 4$; 72 hours: 28% compared with 21%, $n = 5$, control versus PECAM blocked) (Figure 4G).

Image Analysis to Segment Individual Leukocytes in Clusters

The heatmaps made qualitative comparisons easier but were not adequate for quantitatively analyzing the distribution. To facilitate quantitation, a method to segment the images and identify the position of individual cells in relation to the boundary of the brain cortex was developed. Because manual thresholding is unable to separate overlapping cells, a Laplacian of Gaussian filter was used to identify local maxima in the GFP channel corresponding to different cells. With this process (Figure 5), described at length in *Methods and Materials*, the detection of thousands of individual cells in each stitched image can be automated. This method accurately separated >95% of the touching or overlapping cells. The cortical surface was determined using manual thresholding (Figure 5), and the distance of every cell centroid from the cortical surface was recorded, with distance calculated using a standard distance transform (Figure 5).

Disrupting TEM Dramatically Changes the Distribution of Infiltrating Leukocytes

Multiple sections from mice harvested at 24 and 72 hours were processed, both with control or with PECAM function-blocking antibody treatments. The total number of GFP-positive cells recruited to the brain at each time point was not affected by PECAM blockade at either time point (Figure 6A). To examine the distribution in finer detail, each population was binned in 500-μm increments, and the data were normalized to the total number of cells in the population to find the percentage of the total present in each 500-μm bin. Averaging these histograms together for each

FLA 5.6.0 DTD ■ AJPA3771_proof ■ 19 August 2022 ■ 6:39 pm ■ EO: AJPA-D-22-00074

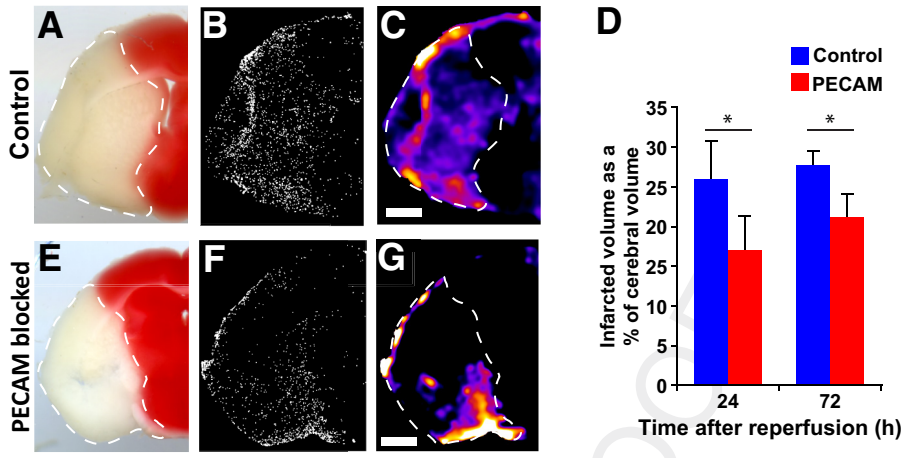

Figure 4 PECAM blockade reduces infarct volume. *LysM-GFP* mice were subjected to transient middle cerebral artery occlusion and reperfused after 90 minutes. Immediately after reperfusion, mice were injected intravenously with either control (**A**–**C**) or PECAM function-blocking antibodies (**E**–**G**). Antibody levels were boosted via i.v. injections every 24 hours to maintain effective levels of the blocking antibody. At either 24 or 72 hours after reperfusion, the mice were injected with a fluorescent-vessel labeling antibody for 30 minutes and then sacrificed. **A**, **B**, **E**, and **F:** Brains were harvested, sliced, and then stained with triphenyltetrazolium chloride, with **dashed lines** denoting the cerebral infarct area (**A** and **E**), and then imaged with fluorescence microscopy (**B** and **F**). **B** and **F:** Representative images of the green fluorescent protein (GFP)-positive leukocyte distribution. **C** and **G:** Heatmap representations of the fluorescence images (from **B** and **F**), with **dashed lines** denoting the cerebral infarct area (from **A** and **E**). The hotter colors (white and yellow) denote higher densities of leukocytes. **D:** Quantitation of the infarct volume of the brains harvested in **A**. **E:** Infarct boundary was measured from both faces of all slices and used to calculate the percentage of the total cerebrum that was infarcted. Data are expressed as means ± SD. $n = 4$ mice at 24 hours; $n = 5$ mice at 72 hours. *$P < 0.05$. Scale bars: 1 mm.

condition allows for direct comparison of the distributions (Figure 6B). Comparison of the averaged distributions in control treatments shows that the population of infiltrating GFP-positive leukocytes shifts toward the subcortex at 72 hours (compared with the control histograms from 24 to 72 hours) (Figure 6B). This shift of the population was statistically significant at both time points, with $P < 0.001$. When PECAM was blocked, the average distance from the surface of the infiltrating leukocyte population was reduced at both 24 hours (0.74 mm compared with 0.47 mm, $n = 4$, control versus PECAM blocked) and 72 hours (1.1 mm compared with 0.77 mm, $n = 5$, control versus PECAM blocked) (Figure 6C).

At both time points, disrupting PECAM function retains the leukocyte population closer to the cortical surface, with the cortex defined as the first millimeter or the first two bins (72% compared with 89% at 24 hours, $n = 4$; and 51% compared with 69% at 72 hours, $n = 5$, control versus PECAM blocked) (Figure 6D).

Neutrophils Are Distributed Heterogeneously across the Infarct Post-Stroke

To specifically visualize the recruitment and distribution of neutrophils, *Catchup-Ly6G* reporter mice, which express tdTomato in all PMNs, were used. All mice used were heterozygous for the *Ly6G* locus so that their PMNs would retain a functional copy of *Ly6G*. Mice were subjected to tMCAO and reperfused after 90 minutes; 72 hours after reperfusion, animals were injected with fluorescent non–function-blocking anti-PECAM antibodies to label the vasculature. Animals were then sacrificed and perfused with phosphate-buffered saline, and brains were harvested, sliced, and then stained with TTC to identify infarcted regions. A series of fluorescence images was acquired across the entire brain slice and were stitched together to create one large high-resolution image of the entire sample. The image was rendered as a heatmap to visualize the density and location of the infiltrating tdTomato-positive PMNs (Figure 7A). At 24 hours, a majority of infiltrating [F7] PMNs are near the cortical surface. By 72 hours, a significant portion of PMNs shift to deeper in the subcortex. To examine the distribution in finer detail, each population was binned in 500-μm increments, and the data were normalized to the total number of PMNs in the population [Q24] to find the percentage of the total present in each 500-μm bin. Averaging these histograms together for each condition allows for direct comparison of the distributions (Figure 7B) ($P < 0.001$, 24 hours population compared with 72 hours). This difference in the PMN population distribution between the two time points shows a more dramatic shift than when LysM-GFP–positive cells (monocytes and PMNs) were examined. Comparison of the average distance from the surface shows that the population of tdTomato-positive PMNs are farther from the surface at 72 hours compared with 24 hours (Figure 7C). At [Q25] 24 hours, a majority of PMNs are located within the cortex, defined as the first millimeter from the brain surface, whereas at 72 hours, significantly fewer PMNs are located within the cortex.

FLA 5.6.0 DTD ■ AJPA3771_proof ■ 19 August 2022 ■ 6:39 pm ■ EO: AJPA-D-22-00074

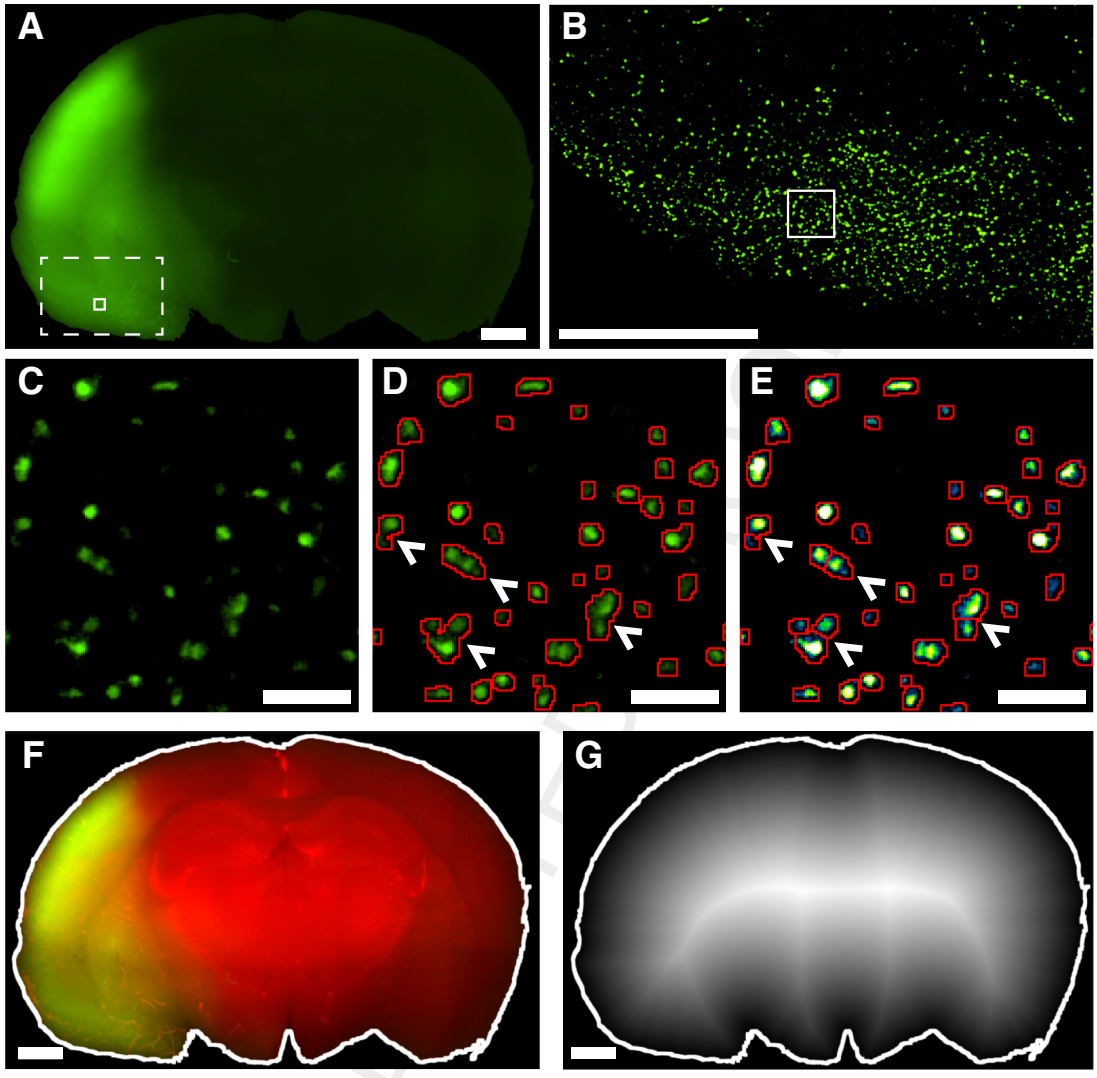

Figure 5 Image processing allows for the segmentation of individual leukocytes and the mapping of their exact position across the infarct. **A:** The raw green fluorescent protein (GFP) channel shows the inherent autofluorescence of the infarct compared with healthy tissue. The **dashed box** denotes the area shown in **B**, and the **solid box** shows the area illustrated in **C**–**E**. **B:** Image after preprocessing for the region marked by the **dashed box** in **A**. Preprocessing removes nonuniform background and enables visualization of cells. **C:** Zoomed in region of the **solid box** in **A** and **B** of the preprocessed image. **D:** Thresholding alone is ineffective in resolving overlapping cells because the region between cells is above the threshold used for segmentation. The **arrowheads** indicate cells that are not effectively delineated from each other. **E:** The image in **D** represents using a heatmap to help visualize local maxima. The Laplacian of Gaussian filter highlights the local maxima, which were used as markers for the marker-based watershed transform for separating overlapping cells. The **arrowheads** indicate cells from **D** that have become effectively delineated from each other after the application of the Laplacian of Gaussian filter and watershed transform. **F:** The brain boundary highlighted in white was determined using both the GFP and vessel channel (shown in red, for better contrast). **G:** Distance transform of the entire brain boundary used to calculate the distance of a given point from the surface, with higher (whiter) intensity denoting greater distance. (Note that this has been done for the entire brain, not just the infarcted side.) The cell centroid position was mapped onto this and used to determine the distance of each cell from the nearest cortical surface. Scale bars: 1 mm (**A**, **B**, **F**, and **G**); 50 μm (**C**–**E**).

Discussion

The progression of stroke therapy into the thrombectomy era opened the reperfusion window for up to 24 hours after stroke occurs.[2,3] The dynamically changing criteria for being eligible for reperfusion therapy suggest that more and more patients will be included for reperfusion therapy.[58] Given the heterogeneous response to thrombectomy and variable outcomes that some patients face,[4,5,59] the authors posit that the understanding of the natural history of I/RI in stroke needs a back-to-basics retooling. Previous work has illustrated that reperfusion itself is heterogeneous in preclinical stroke models.[60] Clinical work has shown that elevated PMN counts, whether they be systemic samples or thrombectomy samples, predict worse outcomes after reperfusion.[61–64] Notably, the failure of clinical trials to translate limitation of leukocyte migration into a positive effect suggests that limiting total PMN infiltration may not be a viable goal to developing new therapies. Accordingly, the authors sought to better define how leukocyte infiltration

FLA 5.6.0 DTD ■ AJPA3771_proof ■ 19 August 2022 ■ 6:39 pm ■ EO: AJPA-D-22-00074

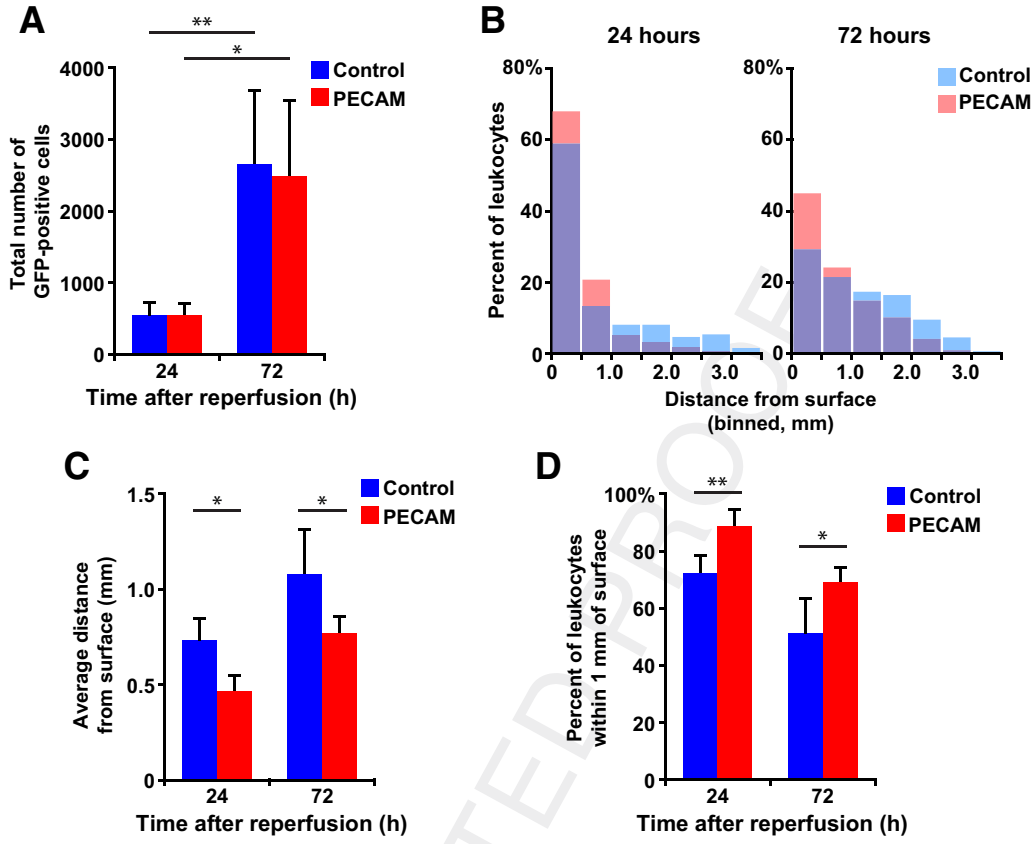

Figure 6 Disrupting PECAM function does not reduce the total number of cells recruited to the infarct but does restrict them closer to the cortical surface. **A:** *LysM-GFP* mice were subjected to transient middle cerebral artery occlusion and reperfused after 90 minutes. Immediately after reperfusion, mice were injected with either control or PECAM function-blocking antibodies as indicated and boosted as described in *Materials and Methods*. Mice were sacrificed at either 24 or 72 hours after reperfusion, and brain slices were processed to identify individual cells as described in Figure 5. **B:** The population data collected in **A** were binned into 500-μm segments and made relative to the total cells for each mouse, averaged for each group (treatment and time point), and binned into 0.5-mm bins. Histograms show the average retention of the populations close to the cortex caused by PECAM blockade at both 24 and 72 hours. This shift was statistically significant at both time points with $P < 0.001$. **C:** The average distance (mm) from the cortical surface for each population was calculated. **D:** Bar graph shows the percentage of GFP-positive leukocytes that were determined to be within the cortex (first mm of the cortical surface) from **A**. Data are expressed as means ± SD. $n = 4$ mice at 24 hours; $n = 5$ mice at 72 hours. $^*P < 0.05$, $^{**}P < 0.01$.

patterns in I/RI occur on a scope that was both precise and holistic. By using PECAM blockade to interrupt TEM, we sought to determine whether altering leukocyte infiltration pattern would reduce stroke volume.

The recruitment of PMNs demonstrates significant spatiotemporal differences across infarcted stroke tissue throughout I/RI and can be modulated by PECAM antibody blockade. The data shown here indicate that tMCAO leukocytes at 24 hours I/RI infiltrate at the cortical surface of the infarct and appear throughout both cortex and subcortex by 72 hours I/RI. At 24 hours I/RI, flow cytometry confirmed that PMNs are the main leukocyte population present in the ischemic hemisphere. The number of leukocytes increased over the 72 hours I/RI, including both PMNs and monocytes. Specific interrogation of PMNs with the use of the *Catchup-Ly6G* mouse model showed that PMNs at 24 hours I/RI infiltrate at the cortical surface of the infarct and appear throughout both cortex and subcortex by 72 hours I/RI, indicating that the spatiotemporal differences throughout I/RI are at least partially driven by PMNs. Unfortunately, the authors were limited in their ability to interrogate the role of PECAM in the *Catchup-Ly6G* model because PECAM does not function the same way in TEM in the C57Bl/6 background.[39] Using this semiautomated method for the quantification of leukocyte number and distance from the surface in an unbiased manner, the authors show PECAM blockade restricts a significant number of leukocytes to the cortex at both 24 hours I/RI and 72 hours I/RI without modulating the total number of leukocytes found in the ischemic hemisphere. Their work also confirms previously reported findings that demonstrated that PECAM blockade also reduced stroke infarct size significantly at both 24 hours I/RI and 72 hours I/RI.[65] Disruption of PECAM binding and signaling, which mediates TEM at a target downstream from prior preclinical stroke targets, limits the progression of PMNs into the infarcted tissue after I/RI. These findings suggest that modulating leukocyte infiltration pattern rather than reducing total leukocyte number can have a protective effect on stroke.

FLA 5.6.0 DTD ■ AJPA3771_proof ■ 19 August 2022 ■ 6:39 pm ■ EO: AJPA-D-22-00074

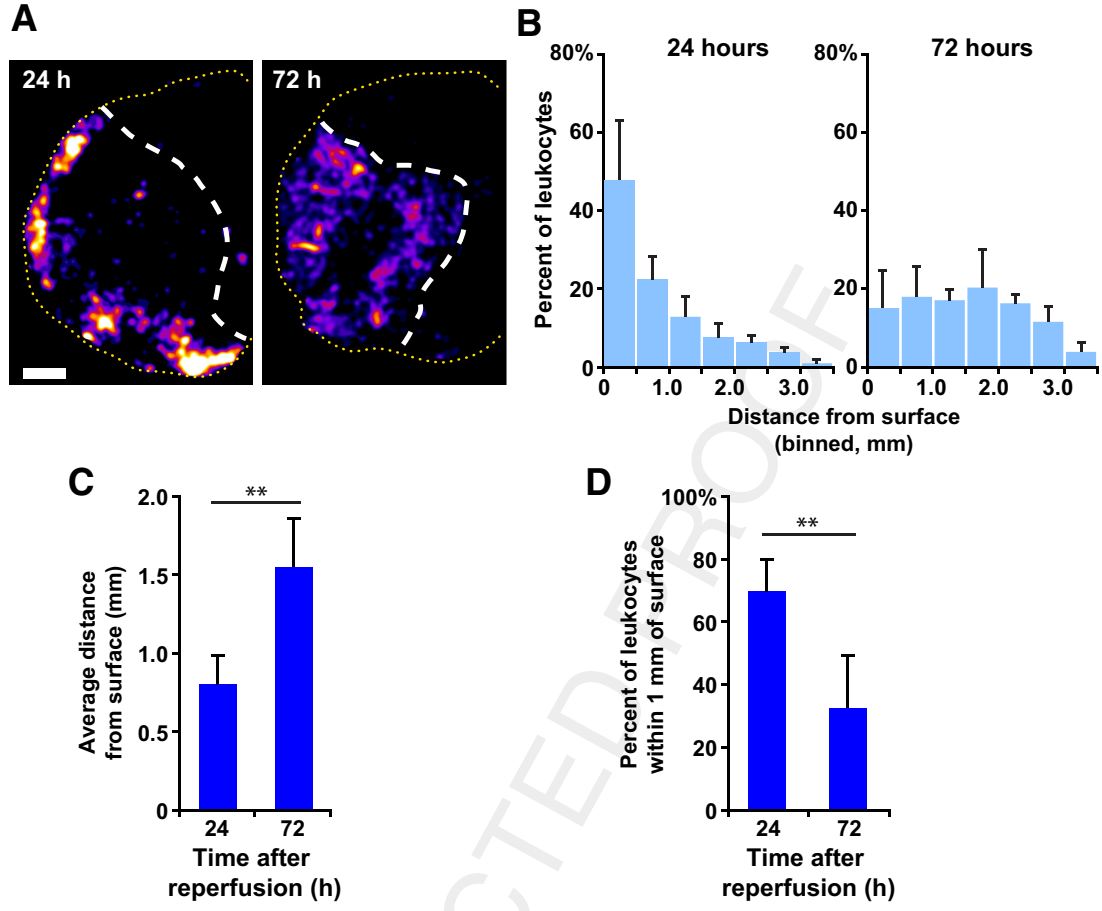

Figure 7 PMN infiltration in various regions of the brain after stroke. **A:** *Catchup-Ly6G* mice were subjected to transient middle cerebral artery occlusion and reperfused after 90 minutes. At either 24 or 72 hours after reperfusion, the mice were injected with a fluorescent-vessel labeling antibody for 30 minutes and sacrificed. Brains were harvested, sliced, stained with triphenyltetrazolium chloride, and then imaged with fluorescence microscopy. Representative images of the tdTomato-positive PMN distribution at 24 hours and 72 hours are shown. **White dashed lines** denote cerebral infarct boundary, and **yellow dashed lines** outline the cortical surface. **B:** The population data collected in **A** were binned into 500-μm segments and made relative to the total cells for each mouse, averaged for each group (24 hours and 72 hours), and binned into 0.5-mm bins. Histograms show the average retention of the populations close to the cortex at both 24 and 72 hours. This shift was statistically significant at both time points, with $P < 0.001$. **C:** The average distance (mm) from the cortical surface for each population was calculated. **D:** Bar graph shows the percentage of tdTomato-positive PMNs that were determined to be within the cortex (first mm of the cortical surface) from **A**. Data are expressed as means ± SD. $n = 4$ mice at 24 hours; $n = 5$ mice at 72 hours. $^{**}P < 0.01$. Scale bar, 1 mm.

Although preclinical studies in rodent models of stroke have identified several molecules in the inflammatory response as potential therapeutic targets,[29,66–68] clinical trials have been unsuccessful.[30–32] These data demonstrate the heterogeneity of leukocyte infiltration in ischemic stroke and raise the possibility that manipulating leukocyte position within the infarct may reduce infarct size. PECAM blockade may be uniquely suited to limit harmful levels of leukocyte recruitment while maintaining some leukocyte recruitment to the parenchyma to participate in the healing process. Previous work on PECAM has previously demonstrated that PECAM limits TEM in multiple preclinical models but has only recently been reported to play role in stroke.[38,39,65,69] This research builds upon prior reports of heterogenous leukocyte spatiotemporal distribution and aligns with preliminary studies conducted in humans.[70–72] Although research has been conducted on the migration of leukocytes and even the effect of PECAM blockade in ischemic stroke, these studies used representative high-resolution confocal imaging to study PMN infiltration.[65,73,74] The authors posit that modulating the natural progression of PMNs from cortical to subcortical compartments may be an alternative approach to reduce the stroke lesion. By using wide-field confocal microscopy and a semiautomated detection process, a cohesive unbiased spatiotemporal image of leukocyte migration into the brain can be generated and used to define the timing and location of PMN infiltration and determine how PECAM blockade and other interventions affect PMN migration. For each sample studied, there is heterogeneity of PMN distribution within the infarct at the same focal plane with some areas of PMN clustering and other areas without PMNs. Heterogeneous PMN infiltration suggests that single-agent antibody blockade will not be sufficient to completely

FLA 5.6.0 DTD ■ AJPA3771_proof ■ 19 August 2022 ■ 6:39 pm ■ EO: AJPA-D-22-00074

block PMN migration. This is not surprising, given that 20% to 30% of leukocytes are known to evade PECAM block in preclinical models at early time points. The restriction of leukocyte infiltration to the cortex via PECAM blockade and heterogeneous infiltration suggests the presence of a preferred TEM zone at the cortical surface. Hypothetically, this TEM zone may be a gateway for entry of leukocytes to the infarcted brain. Accordingly, characterization of this zone and the mechanisms by which PMNs localize to the cortical surface will provide additional targets to inhibit PMN migration and provide insight into optimizing the timing of therapy administration. This may improve the outcomes of TEM blockade therapy in ischemic stroke. In large vessel occlusion (both preclinical and clinical), the deeper subcortical territory may be ischemic first, followed by cortical involvement over time due to decreased collateral blood flow.[75] This level of ischemia may be the prime motivator for leukocyte recruitment as late as 72 hours after the onset of stroke. By reducing leukocyte recruitment to the subcortex, PECAM blockade may reduce stroke volume by limiting secondary injury promoted by inflammatory cell interaction directly with deeply ischemic tissue. White matter, which constitutes a majority of the subcortex, is exquisitely vulnerable to ischemia and may suffer more severe injury than gray matter in stroke.[76]

A known pathologic barrier to reperfusion is the no-reflow phenomenon, where blood flow fails to reperfuse areas of the brain following removal of the obstruction.[77–81] PECAM blockade selectively blocks TEM and does not disrupt leukocyte recruitment or adhesion to the vascular wall. However, the authors do not believe that PECAM blockade contributes to the no-reflow phenomenon because individual blocked leukocytes do not accumulate within the vasculature, but eventually return to the circulation, and the effect of PECAM on transmigration takes place at postcapillary venules that are large enough that transient accumulation of a few PMNs does not obstruct flow. The authors have observed PMN behavior in cerebral vasculature after stroke by intravital microscopy (data not shown) and have not observed blockage of the circulation.

It is also possible that PECAM blockade reduces stroke volume by reducing leukocyte infiltration to the deeply ischemic white matter area and thereby preventing direct communication between hypoxic tissue and inflammatory leukocyte. Alternatively, early recruited leukocytes to the cortex may communicate with deeper ischemic subcortex remotely via spatiotemporally distinct chemokines that have both proresolving and proinflammatory factors. Blocking PECAM early on may shift the most activated and proinflammatory leukocytes from transmigrating at their usual time, thereby reducing subsequent migration of leukocytes into the subcortex. Further studies are needed to better delineate the mechanisms by which how leukocyte recruitment occurs in stroke I/RI and how PECAM can alter this natural history.

Acknowledgments

We thank David Kirchenbuechler and Graham Shekhar for technical advice and support.

Supplemental Data

Supplemental material for this article can be found at *http://doi.org/10.1016/j.ajpath.2022.07.008*.

References

1. Johnston SC, Mendis S, Mathers CD: Global variation in stroke burden and mortality: estimates from monitoring, surveillance, and modelling. Lancet Neurol 2009, 8:345–354
2. Albers GW, Marks MP, Kemp S, Christensen S, Tsai JP, Ortega-Gutierrez S, McTaggart RA, Torbey MT, Kim-Tenser M, Leslie-Mazwi T, Sarraj A, Kasner SE, Ansari SA, Yeatts SD, Hamilton S, Mlynash M, Heit JJ, Zaharchuk G, Kim S, Carrozzella J, Palesch YY, Demchuk AM, Bammer R, Lavori PW, Broderick JP, Lansberg MG: Thrombectomy for stroke at 6 to 16 hours with selection by perfusion imaging. N Engl J Med 2018, 378:708–718
3. Nogueira RG, Jadhav AP, Haussen DC, Bonafe A, Budzik RF, Bhuva P, et al: Thrombectomy 6 to 24 hours after stroke with a mismatch between deficit and infarct. N Engl J Med 2018, 378:11–21
4. Goyal M, Menon BK, van Zwam WH, Dippel DW, Mitchell PJ, Demchuk AM, Davalos A, Majoie CB, van der Lugt A, de Miquel MA, Donnan GA, Roos YB, Bonafe A, Jahan R, Diener HC, van den Berg LA, Levy EI, Berkhemer OA, Pereira VM, Rempel J, Millan M, Davis SM, Roy D, Thornton J, Roman LS, Ribo M, Beumer D, Stouch B, Brown S, Campbell BC, van Oostenbrugge RJ, Saver JL, Hill MD, Jovin TG: Endovascular thrombectomy after large-vessel ischaemic stroke: a meta-analysis of individual patient data from five randomised trials. Lancet 2016, 387:1723–1731
5. Wollenweber FA, Tiedt S, Alegiani A, Alber B, Bangard C, Berrouschot J, et al: Functional outcome following stroke thrombectomy in clinical practice. Stroke 2019, 50:2500–2506
6. Lee JM, Grabb MC, Zipfel GJ, Choi DW: Brain tissue responses to ischemia. J Clin Invest 2000, 106:723–731
7. Nour M, Scalzo F, Liebeskind DS: Ischemia-reperfusion injury in stroke. Interv Neurol 2013, 1:185–199
8. Buck BH, Liebeskind DS, Saver JL, Bang OY, Yun SW, Starkman S, Ali LK, Kim D, Villablanca JP, Salamon N, Razinia T, Ovbiagele B: Early neutrophilia is associated with volume of ischemic tissue in acute stroke. Stroke 2008, 39:355–360
9. Emsley HC, Smith CJ, Gavin CM, Georgiou RF, Vail A, Barberan EM, Hallenbeck JM, del Zoppo GJ, Rothwell NJ, Tyrrell PJ, Hopkins SJ: An early and sustained peripheral inflammatory response in acute ischaemic stroke: relationships with infection and atherosclerosis. J Neuroimmunol 2003, 139:93–101
10. Jin R, Yang G, Li G: Inflammatory mechanisms in ischemic stroke: role of inflammatory cells. J Leukoc Biol 2010, 87:779–789
11. Wang Q, Tang XN, Yenari MA: The inflammatory response in stroke. J Neuroimmunol 2007, 184:53–68
12. Ley K, Laudanna C, Cybulsky MI, Nourshargh S: Getting to the site of inflammation: the leukocyte adhesion cascade updated. Nat Rev Immunol 2007, 7:678–689
13. Muller WA: Mechanisms of transendothelial migration of leukocytes. Circ Res 2009, 105:223–230
14. Butcher EC: Leukocyte-endothelial cell recognition: three (or more) steps to specificity and diversity. Cell 1991, 67:1033–1036
15. Springer TA: Adhesion receptors of the immune system. Nature (London) 1990, 346:425–434

FLA 5.6.0 DTD ■ AJPA3771_proof ■ 19 August 2022 ■ 6:39 pm ■ EO: AJPA-D-22-00074

16. Muller WA: Leukocyte-endothelial cell adhesion molecules in transendothelial migration. Edited by Gallin JI, Snyderman R. In Inflammation: Basic Principles and Clinical Correlates. Philadelphia: Lippincott Williams & Wilkins, 1999. pp. 585–592
17. Ruhnau J, Schulze J, Dressel A, Vogelgesang A: Thrombosis, neuroinflammation, and poststroke infection: the multifaceted role of neutrophils in stroke. J Immunol Res 2017, 2017:5140679
18. Manda-Handzlik A, Demkow U: The brain entangled: the contribution of neutrophil extracellular traps to the diseases of the central nervous system. Cells 2019, 8:1477
19. Enzmann G, Mysiorek C, Gorina R, Cheng YJ, Ghavampour S, Hannocks MJ, Prinz V, Dirnagl U, Endres M, Prinz M, Beschorner R, Harter PN, Mittelbronn M, Engelhardt B, Sorokin L: The neurovascular unit as a selective barrier to polymorphonuclear granulocyte (PMN) infiltration into the brain after ischemic injury. Acta Neuropathol 2013, 125:395–412
20. Otxoa-de-Amezaga A, Gallizioli M, Pedragosa J, Justicia C, Miro-Mur F, Salas-Perdomo A, Diaz-Marugan L, Gunzer M, Planas AM: Location of neutrophils in different compartments of the damaged mouse brain after severe ischemia/reperfusion. Stroke 2019, 50: 1548–1557
21. Shichita T, Ago T, Kamouchi M, Kitazono T, Yoshimura A, Ooboshi H: Novel therapeutic strategies targeting innate immune responses and early inflammation after stroke. J Neurochem 2012, 123(Suppl 2):29–38
22. Neumann J, Henneberg S, von Kenne S, Nolte N, Muller AJ, Schraven B, Gortler MW, Reymann KG, Gunzer M, Riek-Burchardt M: Beware the intruder: real time observation of infiltrated neutrophils and neutrophil-Microglia interaction during stroke in vivo. PLoS One 2018, 13:e0193970
23. Enzmann G, Kargaran S, Engelhardt B: Ischemia-reperfusion injury in stroke: impact of the brain barriers and brain immune privilege on neutrophil function. Ther Adv Neurol Disord 2018, 11. 1756286418794184
24. Norling LV, Spite M, Yang R, Flower RJ, Perretti M, Serhan CN: Cutting edge: humanized nano-proresolving medicines mimic inflammation-resolution and enhance wound healing. J Immunol 2011, 186:5543–5547
25. Dalli J, Serhan CN: Specific lipid mediator signatures of human phagocytes: microparticles stimulate macrophage efferocytosis and pro-resolving mediators. Blood 2012, 120:e60–e72
26. Serhan CN, Levy BD: Resolvins in inflammation: emergence of the pro-resolving superfamily of mediators. J Clin Invest 2018, 128: 2657–2669
27. Kochanek PM, Hallenbeck JM: Polymorphonuclear leukocytes and monocytes/macrophages in the pathogenesis of cerebral ischemia and stroke. Stroke 1992, 23:1367–1379
28. Connolly ES Jr, Winfree CJ, Springer TA, Naka Y, Liao H, Yan SD, Stern DM, Solomon RA, Gutierrez-Ramos JC, Pinsky DJ: Cerebral protection in homozygous null ICAM-1 mice after middle cerebral artery occlusion. Role of neutrophil adhesion in the pathogenesis of stroke. J Clin Invest 1996, 97:209–216
29. Harris AK, Ergul A, Kozak A, Machado LS, Johnson MH, Fagan SC: Effect of neutrophil depletion on gelatinase expression, edema formation and hemorrhagic transformation after focal ischemic stroke. BMC Neurosci 2005, 6:49
30. Enlimomab Acute Stroke Trial Investigators: Use of anti-ICAM-1 therapy in ischemic stroke: results of the Enlimomab Acute Stroke Trial. Neurology 2001, 57:1428–1434
31. Fu Y, Zhang N, Ren L, Yan Y, Sun N, Li YJ, Han W, Xue R, Liu Q, Hao J, Yu C, Shi FD: Impact of an immune modulator fingolimod on acute ischemic stroke. Proc Natl Acad Sci U S A 2014, 111: 18315–18320
32. Elkins J, Veltkamp R, Montaner J, Johnston SC, Singhal AB, Becker K, Lansberg MG, Tang W, Chang I, Muralidharan K, Gheuens S, Mehta L, Elkind MSV: Safety and efficacy of natalizumab in patients with acute ischaemic stroke (ACTION): a randomised, placebo-controlled, double-blind phase 2 trial. Lancet Neurol 2017, 16:217–226
33. Muller WA, Ratti CM, McDonnell SL, Cohn ZA: A human endothelial cell-restricted, externally disposed plasmalemmal protein enriched in intercellular junctions. J Exp Med 1989, 170: 399–414
34. Mamdouh Z, Chen X, Pierini LM, Maxfield FR, Muller WA: Targeted recycling of PECAM from endothelial cell surface-connected compartments during diapedesis. Nature 2003, 421:748–753
35. Muller WA, Weigl SA, Deng X, Phillips DM: PECAM-1 is required for transendothelial migration of leukocytes. J Exp Med 1993, 178: 449–460
36. Muller WA: PECAM: regulating the start of diapedesis. Edited by Ley K. In Adhesion Molecules: Function and Inhibition. Basel: Birkhauser Verlag AG, 2007. pp. 201–220
37. Wimmer I, Tietz S, Nishihara H, Deutsch U, Sallusto F, Gosselet F, Lyck R, Muller WA, Lassmann H, Engelhardt B: PECAM-1 stabilizes blood-brain barrier integrity and favors paracellular T-cell diapedesis across the blood-brain barrier during neuroinflammation. Front Immunol 2019, 10:711
38. Dasgupta B, Chew T, deRoche A, Muller WA: Blocking platelet/endothelial cell adhesion molecule 1 (PECAM) inhibits disease progression and prevents joint erosion in established collagen antibody-induced arthritis. Exp Mol Pathol 2010, 88:210–215
39. Sullivan DP, Watson RL, Muller WA: 4D intravital microscopy uncovers critical strain differences for the roles of PECAM and CD99 in leukocyte diapedesis. Am J Physiol Heart Circ Physiol 2016, 311: H621–H632
40. Dalal PJ, Sullivan DP, Weber EW, Sacks DB, Gunzer M, Grumbach IM, Heller Brown J, Muller WA: Spatiotemporal restriction of endothelial cell calcium signaling is required during leukocyte transmigration. J Exp Med 2021, 218:e20192378
41. Hasenberg A, Hasenberg M, Mann L, Neumann F, Borkenstein L, Stecher M, Kraus A, Engel DR, Klingberg A, Seddigh P, Abdullah Z, Klebow S, Engelmann S, Reinhold A, Brandau S, Seeling M, Waisman A, Schraven B, Gothert JR, Nimmerjahn F, Gunzer M: Catchup: a mouse model for imaging-based tracking and modulation of neutrophil granulocytes. Nat Methods 2015, 12:445–452
42. Engel O, Kolodziej S, Dirnagl U, Prinz V: Modeling stroke in mice - middle cerebral artery occlusion with the filament model. J Vis Exp 2011:2423
43. Sommer CJ: Ischemic stroke: experimental models and reality. Acta Neuropathol 2017, 133:245–261
44. Bertrand L, Dygert L, Toborek M: Induction of ischemic stroke and ischemia-reperfusion in mice using the middle artery occlusion technique and visualization of infarct area. J Vis Exp 2017: 54805
45. Bogen S, Pak J, Garifallou M, Deng X, Muller WA: Monoclonal antibody to murine PECAM-1 [CD31] blocks acute inflammation in vivo. J Exp Med 1994, 179:1059–1064
46. Woodfin A, Voisin MB, Beyrau M, Colom B, Caille D, Diapouli FM, Nash GB, Chavakis T, Albelda SM, Rainger GE, Meda P, Imhof BA, Nourshargh S: The junctional adhesion molecule JAM-C regulates polarized transendothelial migration of neutrophils in vivo. Nat Immunol 2011, 12:761–769
47. Schneider CA, Rasband WS, Eliceiri KW: NIH Image to ImageJ: 25 years of image analysis. Nat Methods 2012, 9:671–675
48. van der Walt S, Schonberger JL, Nunez-Iglesias J, Boulogne F, Warner JD, Yager N, Gouillart E, Yu T; c scikit-image contributors: scikit-image: image processing in Python. PeerJ 2014, 2:e453
49. Russell RA, Adams NM, Stephens DA, Batty E, Jensen K, Freemont PS: Segmentation of fluorescence microscopy images for quantitative analysis of cell nuclear architecture. Biophys J 2009, 96: 3379–3389
50. Parvati K, Rao BSP, Mariya Das M: Image segmentation using gray-scale morphology and marker-controlled watershed transformation. Discrete Dyn Nat Soc 2008, 2008. Article ID 384346

FLA 5.6.0 DTD ■ AJPA3771_proof ■ 19 August 2022 ■ 6:39 pm ■ EO: AJPA-D-22-00074

51. Kong H, Akakin HC, Sarma SE: A generalized Laplacian of Gaussian filter for blob detection and its applications. IEEE Trans Cybern 2013, 43:1719–1733
52. Abdolhoseini M, Kluge MG, Walker FR, Johnson SJ: Segmentation of heavily clustered nuclei from histopathological images. Sci Rep 2019, 9:4551
53. Neubeck A, Van Gool L: Efficient non-maximum suppression. Los Alamitos, CA, IEEE Computer Society, 2006. pp. 850–855. 18th International Conference on Pattern Recognition (ICPR'06)
54. Paglieroni DW: Distance transforms: properties and machine vision applications. CVGIP Graph Models Image Process 1992, 54:56–74
55. Sharma S, Ifergan I, Kurz JE, Linsenmeier RA, Xu D, Cooper JG, Miller SD, Kessler JA: Intravenous immunomodulatory nanoparticle treatment for traumatic brain injury. Ann Neurol 2020, 87:442–455
56. Seidman MA, Chew TW, Schenkel AR, Muller WA: PECAM-independent thioglycollate peritonitis is associated with a locus on murine chromosome 2. PLoS One 2009, 4:e4316
57. Schenkel AR, Chew TW, Chlipala E, Harbord MW, Muller WA: Different susceptibilities of PECAM-deficient mouse strains to spontaneous idiopathic pneumonitis. Exp Mol Pathol 2006, 81:23–30
58. Molina CA, Saver JL: Extending reperfusion therapy for acute ischemic stroke: emerging pharmacological, mechanical, and imaging strategies. Stroke 2005, 36:2311–2320
59. Aly M, Abdalla RN, Batra A, Shaibani A, Hurley MC, Jahromi BS, Potts MB, Ansari SA: Follow-up neutrophil-lymphocyte ratio after stroke thrombectomy is an independent biomarker of clinical outcome. J Neurointerv Surg 2021, 13:609–613
60. Beckmann L, Zhang X, Nadkarni NA, Cai Z, Batra A, Sullivan DP, Muller WA, Sun C, Kuranov R, Zhang HF: Longitudinal deep-brain imaging in mouse using visible-light optical coherence tomography through chronic microprism cranial window. Biomed Opt Express 2019, 10:5235–5250
61. He W, Ruan Y, Yuan C, Cheng Q, Cheng H, Zeng Y, Chen Y, Huang G, Chen H, He J: High neutrophil-to-platelet ratio is associated with hemorrhagic transformation in patients with acute ischemic stroke. Front Neurol 2019, 10:1310
62. Ross AM, Hurn P, Perrin N, Wood L, Carlini W, Potempa K: Evidence of the peripheral inflammatory response in patients with transient ischemic attack. J Stroke Cerebrovasc Dis 2007, 16:203–207
63. Kim J, Song TJ, Park JH, Lee HS, Nam CM, Nam HS, Kim YD, Heo JH: Different prognostic value of white blood cell subtypes in patients with acute cerebral infarction. Atherosclerosis 2012, 222:464–467
64. Kumar AD, Boehme AK, Siegler JE, Gillette M, Albright KC, Martin-Schild S: Leukocytosis in patients with neurologic deterioration after acute ischemic stroke is associated with poor outcomes. J Stroke Cerebrovasc Dis 2013, 22:e111–e117
65. Winneberger J, Schols S, Lessmann K, Randez-Garbayo J, Bauer AT, Mohamud Yusuf A, Hermann DM, Gunzer M, Schneider SW, Fiehler J, Gerloff C, Gelderblom M, Ludewig P, Magnus T: Platelet endothelial cell adhesion molecule-1 is a gatekeeper of neutrophil transendothelial migration in ischemic stroke. Brain Behav Immun 2021, 93:277–287
66. Hughes PM, Allegrini PR, Rudin M, Perry VH, Mir AK, Wiessner C: Monocyte chemoattractant protein-1 deficiency is protective in a murine stroke model. J Cereb Blood Flow Metab 2002, 22:308–317
67. Denes A, Ferenczi S, Halasz J, Kornyei Z, Kovacs KJ: Role of CX3CR1 (fractalkine receptor) in brain damage and inflammation induced by focal cerebral ischemia in mouse. J Cereb Blood Flow Metab 2008, 28:1707–1721
68. Yrjanheikki J, Tikka T, Keinanen R, Goldsteins G, Chan PH, Koistinaho J: A tetracycline derivative, minocycline, reduces inflammation and protects against focal cerebral ischemia with a wide therapeutic window. Proc Natl Acad Sci U S A 1999, 96: 13496–13500
69. Liao F, Ali J, Greene T, Muller WA: Soluble domain 1 of platelet-endothelial cell adhesion molecule (PECAM) is sufficient to block transendothelial migration in vitro and in vivo. J Exp Med 1997, 185: 1349–1357
70. Lindsberg PJ, Carpen O, Paetau A, Karjalainen-Lindsberg ML, Kaste M: Endothelial ICAM-1 expression associated with inflammatory cell response in human ischemic stroke. Circulation 1996, 94: 939–945
71. Hallenbeck JM, Dutka AJ, Tanishima T, Kochanek PM, Kumaroo KK, Thompson CB, Obrenovitch TP, Contreras TJ: Polymorphonuclear leukocyte accumulation in brain regions with low blood flow during the early postischemic period. Stroke 1986, 17: 246–253
72. Barone FC, Hillegass LM, Price WJ, White RF, Lee EV, Feuerstein GZ, Sarau HM, Clark RK, Griswold DE: Polymorphonuclear leukocyte infiltration into cerebral focal ischemic tissue: myeloperoxidase activity assay and histologic verification. J Neurosci Res 1991, 29:336–345
73. Ishikawa M, Vowinkel T, Stokes KY, Arumugam TV, Yilmaz G, Nanda A, Granger DN: CD40/CD40 ligand signaling in mouse cerebral microvasculature after focal ischemia/reperfusion. Circulation 2005, 111:1690–1696
74. Yilmaz G, Arumugam TV, Stokes KY, Granger DN: Role of T lymphocytes and interferon-gamma in ischemic stroke. Circulation 2006, 113:2105–2112
75. Liebeskind DS: Collateral circulation. Stroke 2003, 34:2279–2284
76. Wang Y, Liu G, Hong D, Chen F, Ji X, Cao G: White matter injury in ischemic stroke. Prog Neurobiol 2016, 141:45–60
77. Garcia JH, Liu KF, Yoshida Y, Lian J, Chen S, del Zoppo GJ: Influx of leukocytes and platelets in an evolving brain infarct (Wistar rat). Am J Pathol 1994, 144:188–199
78. Mori E, del Zoppo GJ, Chambers JD, Copeland BR, Arfors KE: Inhibition of polymorphonuclear leukocyte adherence suppresses no-reflow after focal cerebral ischemia in baboons. Stroke 1992, 23: 712–718
79. Schmid-Schonbein GW: Capillary plugging by granulocytes and the no-reflow phenomenon in the microcirculation. Fed Proc 1987, 46: 2397–2401
80. El Amki M, Gluck C, Binder N, Middleham W, Wyss MT, Weiss T, Meister H, Luft A, Weller M, Weber B, Wegener S: Neutrophils obstructing brain capillaries are a major cause of no-reflow in ischemic stroke. Cell Rep 2020, 33:108260
81. del Zoppo GJ, Schmid-Schonbein GW, Mori E, Copeland BR, Chang CM: Polymorphonuclear leukocytes occlude capillaries following middle cerebral artery occlusion and reperfusion in baboons. Stroke 1991, 22:1276–1283

FLA 5.6.0 DTD ■ AJPA3771_proof ■ 19 August 2022 ■ 6:39 pm ■ EO: AJPA-D-22-00074